

Quiescent times in Gamma-Ray-Bursts: evidence of a dormant inner engine

Alessandro Drago^{1,2}, Giuseppe Pagliara^{3,2}

¹*Dipartimento di Fisica, Università di Ferrara, 44100 Ferrara, Italy*

²*INFN, Sezione di Ferrara, 44100 Ferrara, Italy and*

³*Dipartimento di Fisica, Politecnico di Torino, 10129 Torino, Italy*

The time structure of Gamma Ray Bursts (GRBs) is usually complex and it often displays several short pulses separated by time intervals lasting from fractions of second to several ten of seconds. A previous statistical analysis [1] has shown that there are three time-scales in the GRB light curves: the shortest one is the variability scale determining the pulses' durations and the intervals between pulses; the largest one describes the total duration of the burst and finally, an intermediate time scale is associated with long periods within the bursts having no activity, the so called *quiescent times*. Here we show, through a statistical analysis, that if a quiescent time longer than a few ten of seconds is present in the light curve then the pre-quiescence and the post-quiescence emissions have similar variability scales, but the post-quiescence emission is longer and only marginally softer than the pre-quiescence emission. The similarities between the first and the second emission periods strongly suggest that both emissions are produced by the same mechanism and that long quiescent times are generated by a turning off of the inner engine rather than by stochastic modulation of a continuous wind [2].

We have performed a statistical analysis of the time intervals Δt between adjacent peaks using the Li & Fenimore peak finding algorithm [3] and borrowing from Nakar & Piran [4] the definition of active periods separated by Quiescent Times (QTs). In Fig. 1 we show an example of burst where the previous quantities are illustrated. We have applied this analysis to all the light curves of the BATSE catalogue.

In a first investigation we have merged all the bursts of the catalogue into one sample from which we compute the cumulative probability $c(\Delta t)$ of time intervals Δt which are not QTs i.e. of the time intervals within each active period. In Fig. 2a, we show that $c(\Delta t)$ is well described by a log-normal distribution. In Fig. 2b, the histogram of QTs is displayed together with a log-normal distribution. As already observed by previous authors [1], there is an evident deviation of the data points respect to the log-normal distribution for time intervals longer than a few seconds, indicating an excess of long Δt . In Fig. 2c we show a power law fit of the tail of the QTs distribution which displays a very good agreement with the data, as already observed by Quilligan *et al.* [5]. The physical interpretation of this distribution will be discussed later. Finally, in Fig. 2d we show a correlation function, indicating the probability of finding at least 2 QTs longer than ΔT in a same GRB. As shown in the figure this probability rapidly decreases and it essentially vanishes for $\Delta T > 40$ s.

We can now define a subsample of the BATSE catalogue composed of all the bursts having a QT longer than 40 s. In Fig. 2a we also show the distribution of Δt within the subsample. The distributions of the full BATSE catalogue and of the subsample are essentially equal. This indicates that the subsample is not composed of bursts having an anomalously large redshift because instead all time scales within the subsample would be homogeneously dilated.

In our analysis we will now concentrate on the subsample. From the result of Fig. 2d, the bursts of the subsample contain only one long QT and it is therefore possible to divide each burst into a pre-quiescence and a post-quiescence emission (PreQE, PostQE) of which we will compare the temporal and spectral structure.

In Fig. 3 we display the cumulative distributions $c_1(\Delta t)$ and $c_2(\Delta t)$ within each of the two emission periods. The two distributions are very similar. The χ^2 -test provides a significance of 34% that the two data sets are drawn from the same distribution function. Let us remind that within the internal-external shocks model [6, 7], external shocks produce emissions lacking the short time scale variability produced by internal shocks [8]. The result of Fig. 3 rules out a scenario in which PostQE is dominated by external shocks and PreQE by internal shocks. This in turn excludes the possibility of associating the QTs with the time needed to the jet to reach and interact with the interstellar medium. Clearly enough, the statistical analysis we are presenting does not rule out the existence of specific GRBs in which the second episode is indeed associated with external shocks. For instance GRB960530 and GRB980125 are examples of bursts in which PostQE has a smoother morphology and a softer spectral evolution than PreQE [9].

We perform now a statistical analysis of the durations $D1$ and $D2$ of the two emission periods. As shown in Fig. 4a, the two data sets are well fitted by two log-normal distributions (the Kolmogorov-Smirnov test provides a significance of $\sim 90\%$). The two distributions have different mean values ($D1_{ave} \sim 4.9s$, $D2_{ave} \sim 11.7s$) and almost identical standard deviations ($\sigma_1 = 0.47$, $\sigma_2 = 0.48$). We address now the following question: is the longer duration of PostQE a manifestation of a progressive increase in the active periods' durations during the burst? To answer the question we have repeated the previous analysis by dividing PreQE and PostQE each in two parts, using the longest QT within each emission as a divider. The distributions of the duration of all parts are shown in Fig. 4b. The durations of the

two parts within each emission period share the same distribution (the χ^2 -test provides significances larger than 50% in both cases) but, in agreement with the previous findings, the average durations of the two parts of PostQE are longer than the two parts of PreQE. Therefore, the longer duration of PostQE cannot be attributed to a continuous modification of the emission but is a specific feature of the second part of the GRB.

To estimate the emitted energy during PreQE and PostQE we have analyzed the hardness ratios, defined as the ratios between the photon counts in two BATSE channels (the second and the third in our case). The average hardness of PostQE turns out to be only marginally smaller ($\sim 20\%$) than the average hardness of PreQE. Since $D2_{ave} \sim 2.4D1_{ave}$, the total energy emitted during PostQE is about a factor of 2 larger than the one emitted during PreQE.

Let us now discuss how our results provide new constraints on models of GRBs light curves. As observed by Ramirez et al. [2], within the internal shocks model it is possible to explain the QTs either as a turn-off of the inner engine or as a modulation of a continuous relativistic wind emitted by the inner engine. Both hypothesis are consistent with the result of Fig. 3. However, in a scenario in which QTs are stochastically generated by modulating a continuous wind the average durations of the two episodes should be essentially equal, since no new dimensional scale is introduced. Our results suggests instead that, although the mechanism of emission in the two episodes is probably the same (Fig. 3), the duration of the second episode is larger (Fig. 4a). Moreover, within the wind modulation model, in order to produce a QT lasting T , the source must emit a series of shell [2] during about $2T$. In our analysis we have observed QTs lasting a few hundreds seconds. These QTs have to be corrected taking into account the average redshift of the BATSE catalogue [10], $z_{ave} \sim 2$, but even after this renormalization QTs lasting one minute or more are not too rare. Since a jet emitting continuously during a couple of minutes can hardly be obtained using the existing models of the inner engine, we conclude that long QTs most probably correspond to periods of inactivity of the inner engine. On the other hand, it is possible that the wind modulation mechanism is responsible for the short QTs occurring within the two emission periods, as suggested by Fig. 4b where it is shown that the durations of the two parts of a single emission period have the same distribution, as one would expect if the mechanism responsible for the short QTs is stochastic.

Let us now discuss how to generate dormant periods using various models of the GRBs inner engine. Within the most popular model, the Collapsar model [11], there are two possible scenarios: a temporary interruption of the jet produced by Kelvin-Helmhotz instabilities [12] or the fragmentation of the collapsing stellar core before its merging with the black hole [13]. Although in both scenarios it can be possible to produce long QTs it is not clear how to associate the two different durations of PreQE and PostQE with two dimensional parameters of the model. For instance, in the scenario proposed by King *et al.* [13] the average mass of the second fragment should be larger than that of the first fragment.

Another model for the inner engine is based on the conversion of a metastable hadronic star into a star containing quark matter [14, 15, 16]. In the last years the possibility of forming a diquark condensate at the center of a compact star has been widely discussed in the literature [17]. The formation of a color superconducting quark core can increase the energy released by a significant amount [18]. It has also been shown that the conversion from normal to gapped quark matter goes through a first order transition [19]. It is therefore tempting to associate PreQE with the transition from hadronic to normal quark matter and PostQE with the formation of the superconducting phase [20]. In this scenario the two dimensional scales regulating the durations of PreQE and PostQE are the energies released in the two transitions. Finally, let us remark that the Pareto-Levi tail fitting the long QTs distribution can originate from a superposition of exponential distributions with different time decays [21]. In the quark deconfinement model, the different decay times are associated with slightly different masses of the metastable compact star.

A possible signature of the models in which the inner engine goes dormant would be the detection of external shock emissions at the end of both PreQE and PostQE, indicating that the two emissions are physically disconnected. If the interpretation based on the quark deconfinement model is correct then the GRBs data analysis provides very stringent bounds on the physics of high density matter.

It is a pleasure to thank Filippo Frontera and Enrico Montanari for many useful suggestions and for help in the data analysis.

[1] Nakar E., Piran T., Time scales in long GRBs. *Mon. Not. Roy. Astron. Soc.* **331**, 40-44 (2002).
 [2] Ramirez-Ruiz E., Merloni A., Rees M.J., Quiescent times in gamma-ray bursts: II. Dormant periods in the central engine? *Mon. Not. Roy. Astron. Soc.* **324** 1147-1158 (2001).
 [3] Li H., Fenimore E., Log-normal Distributions in Gamma-Ray Burst Time Histories. *Astrophys. J.* **469**, L115-L118 (1996).
 [4] Nakar E., Piran T., Temporal properties of short GRBs *Mon. Not. Roy. Astron. Soc.* **330**, 920-926 (2002).

- [5] Quilligan F., McBreen B., Hanlon L., McBreen S., Hurley K.J., Watson D., Temporal properties of gamma-ray bursts as signatures of jets from the central engine *Astron. & Astrophys.* **385**, 377-398 (2002).
- [6] Piran T., The Physics of Gamma-Ray-Bursts, *Rev.Mod.Phys.* **76** 1143-1210 (2004).
- [7] Zhang B., Meszaros P., Gamma-Ray Bursts: Progress, problems & prospects, *Int.J.Mod.Phys. A* **19** 2385-2472 (2004).
- [8] Sari R., Piran T., Variability in Gamma-Ray Bursts: A Clue, *Astrophys.J.* **485**, 270-273 (1997).
- [9] Hakkila J., Giblin T.W., Quiescent Burst Evidence for Two Distinct GRB Emission Components, *Astrophys.J.* **610**, 361-367 (2004).
- [10] Piran T., Gamma-Ray Bursts and the Fireball Model, *Phys.Rept.* **314** 575-667 (1999).
- [11] MacFadyen A.L., Woosley S.E., Collapsars: Gamma-Ray Bursts and explosions in “failed supernovae”, *Astrophys.J.* **524**, 262-289 (1999).
- [12] Woosley S.E., Zhang W., Heger A., The Central Engines og Gamma-Ray-Bursts, *AIP Conference Proceedings* **662**, 185-192 (2003).
- [13] King A., O’Brien P.T., Goad M.R., Osborne J., Olsson E., Page K., Gamma-ray bursts: Restarting the Engine, *Astrophys.J.* **630**, L113-L116 (2005).
- [14] Cheng K.S., Dai Z.G., Conversion of neutron stars to strange stars as an origin of gamma-ray bursts, *Phys.Rev.Lett.* **77** 1210-1213 (1996).
- [15] Bombaci I., Datta B., Conversion of neutron stars to strange stars as the central engine of gamma-ray bursts, *Astrophys.J.* **530** L69 (2000).
- [16] Berezhiani Z. *et al*, Gamma Ray Bursts from delayed collapse of neutron stars to quark matter stars, *Astrophys.J.* **586**, 1250-1253 (2003).
- [17] Rajagopal K., Wilczek F., The Condensed Matter Physics of QCD, hep-ph/0011333.
- [18] Drago. A, Lavagno A., Pagliara G., Effects of color superconductivity on the structure and formation of compact stars, *Phys.Rev.* **D69**, 057505 (2004).
- [19] Ruster S.B. , Werth V., Buballa M., Shovkovy I.A., Rischke D.H., The phase diagram of neutral quark matter: The effect of neutrino trapping hep-ph/0509073.
- [20] Drago. A, Lavagno A., Pagliara G., Gamma Ray Bursts and the transition to Quark Matter in Compact Stars, astro-ph/0510018, Proceedings QM2005, August 2005 Budapest.
- [21] Wheatland M.S., The origin of the solar flare waiting-time distribution, *Astrophys. J.* **536** L109 L112 (2000).

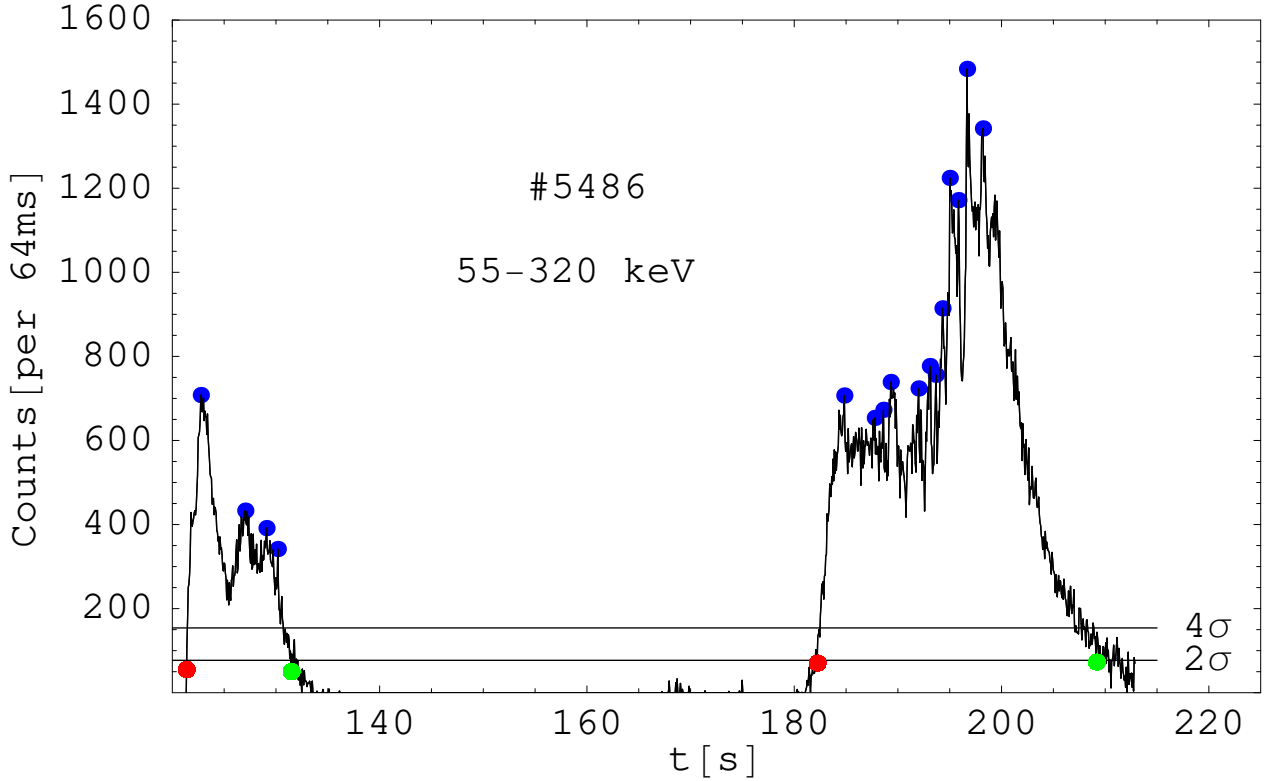


FIG. 1: **Light curve of a typical GRB** Time profile of BATSE burst #5486 in the energy range $55\text{Kev} < E < 320\text{Kev}$. For each light curve, the background is first determined using a linear fit and then subtracted from the data. The signal is extracted taking as initial and final bins the ones with counts above 2σ . The active periods are defined as periods in which bins with counts exceeding 4σ are present. Active periods begin (red dots) and end (green dots) when the signal drops below 2σ . Within each active period we search for peaks using the Li & Fenimore peak finding algorithm [3]: indicating with C_p the counts of a candidate peak and with C_1 and C_2 the counts in the bins to the left and to the right of the candidate, a “true” peak must satisfy the relations $C_p - C_{1,2} \geq Nvar\sqrt{C_p}$, where $Nvar = 5$ in our analysis. The true peaks are indicated by the blue points.

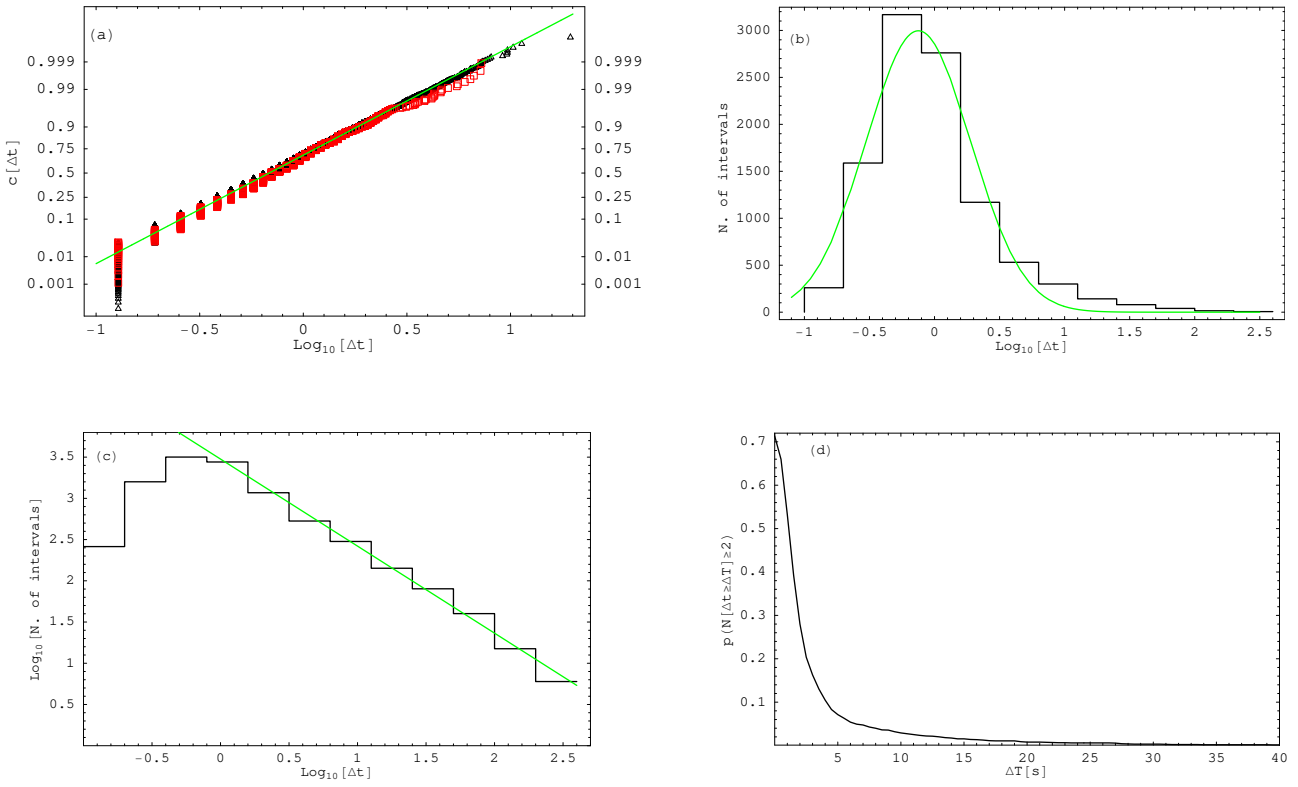


FIG. 2: **Analysis of time intervals between peaks** **a** The cumulative distribution of time intervals Δt which are not QTs (black triangles), is compared with its best fit log-normal distribution (solid green line). The data come from the full BATSE sample after eliminating bursts displaying data gaps. The red boxes correspond to the cumulative distribution of Δt taken from the subsample of bursts with a QT longer than 40s (see text). **b** Histogram of the QTs and its log-normal fit (solid green line). **c** Histogram of QTs and power-low fit of its tail (solid green line). The fit is based only on QTs longer than 40s. **d** Frequency of bursts containing at least two QTs longer than ΔT .

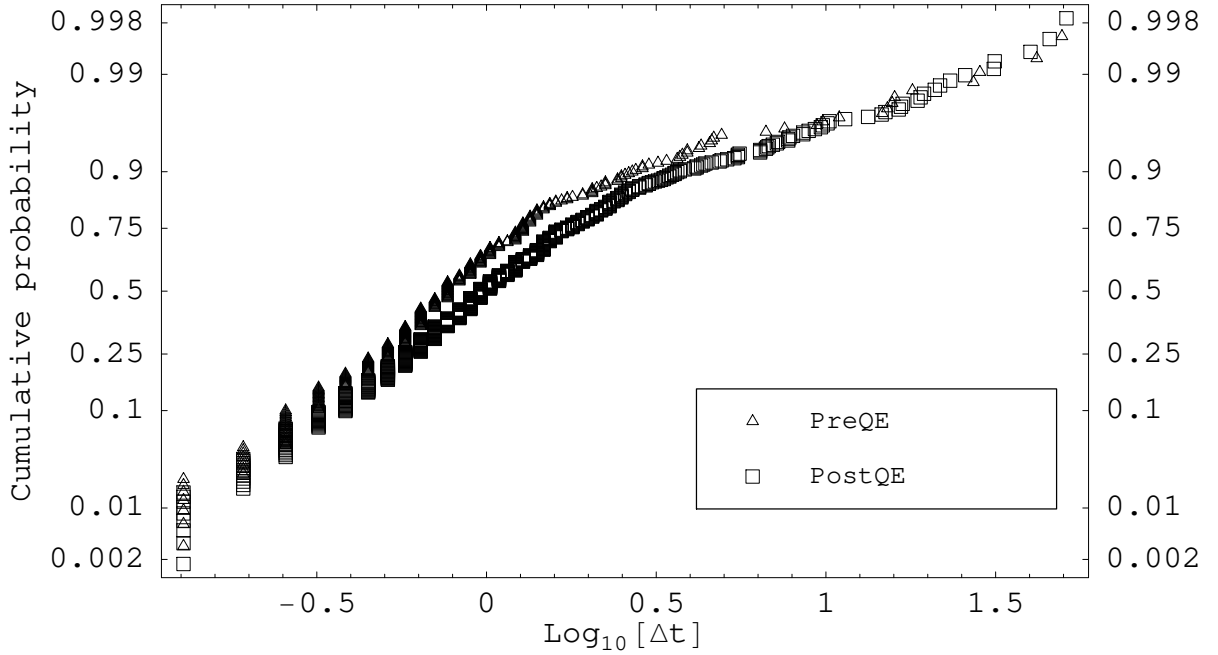


FIG. 3: **Analysis of time intervals between peaks within the two emission periods** The cumulative distributions of Δt are shown for the two emission episodes, PreQE and PostQE. At variance with Fig. 2, all Δt are considered, including QTs.

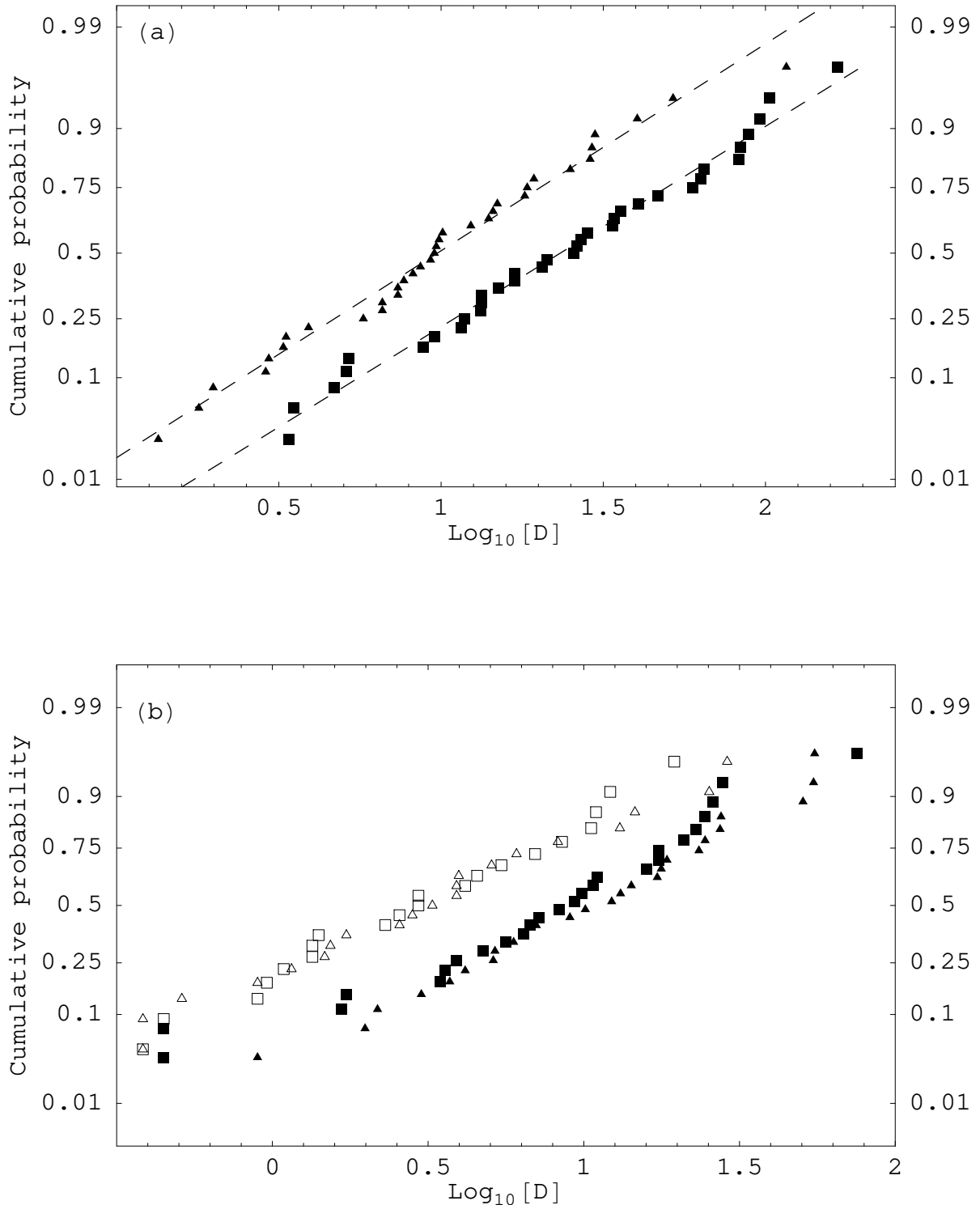


FIG. 4: **Analysis of the durations D of the two emission periods** **a** Cumulative distributions of durations of PreQE (triangles) and of PostQE (boxes) and their best-fit log-normal distributions (dotted lines). **b** Cumulative distributions of durations of the first and second part of PreQE (empty triangles and boxes) and of PostQE (filled triangles and boxes).